Effect of Velocity Ratio on the Streamwise Vortex Structures in the Wake of a Stack

M.S. ADARAMOLA[1]**, D. SUMNER**[2]**, D.J. BERGSTROM**[2]

[1]*Division of Environmental Engineering, University of Saskatchewan*

[2]*Department of Mechanical Engineering, University of Saskatchewan*

57 Campus Drive, Saskatoon, Saskatchewan, Canada, S7N 5A9, david.sumner@usask.ca

Abstract. The time-averaged velocity and streamwise vorticity fields within the wake of a short stack were investigated in a low-speed wind tunnel using a seven-hole pressure probe. The stack was mounted normal to a ground plane and was partially immersed in a flat-plate turbulent boundary layer. The jet-to-cross-flow velocity ratio was varied from $R = 0$ to 3, which covered the downwash, cross-wind-dominated and jet-dominated flow regimes. In the downwash and cross-wind-dominated flow regimes, two pairs of counter-rotating streamwise vortex structures were identified within the stack wake. The tip-vortex pair and base-vortex pair were similar to those found in the wake of a finite circular cylinder, located close to the free end and the base of the stack, respectively. In the jet-dominated flow regime, a third pair of streamwise vortex structures was observed, referred to as the jet-wake vortex pair, which occurred within the jet-wake region above the free end of the stack. The jet-wake vortex pair has the same orientation as the base vortex pair and is associated with the jet rise.

Key words: bluff body aerodynamics, turbulent wake, turbulent jet, stack, vortex structures.

1. Introduction

The separated flow field of a finite circular cylinder mounted normal to a ground plane is very complex and strongly three-dimensional, due to the flow around the base and over the free end [1, 9, 11, 12]. There are marked changes in the near-wake flow structure along the cylinder height and these changes are strongly influenced by the cylinder's aspect ratio, AR (= H/D, where H and D are the height and diameter of the cylinder, respectively), and the relative thickness of the flat-plate boundary layer on the ground plane, δ/H (where δ is the boundary layer thickness at the location of the cylinder). When the AR exceeds a critical value (which depends on δ/H and other parameters), two pairs of streamwise vortex structures are found within the wake of the finite circular cylinder [11, 12]. The first pair, called the tip vortex structures, is formed close to the free end, while the second pair, known as the base vortex structures, is found within the flat-plate boundary layer on the ground plane closer to the base of the cylinder. The tip vortex structures interact in a complex manner with Kármán vortex shedding from the sides of the cylinder, and are responsible for a downward-directed local velocity field near the free end referred to as "downwash." Similarly, an "up-
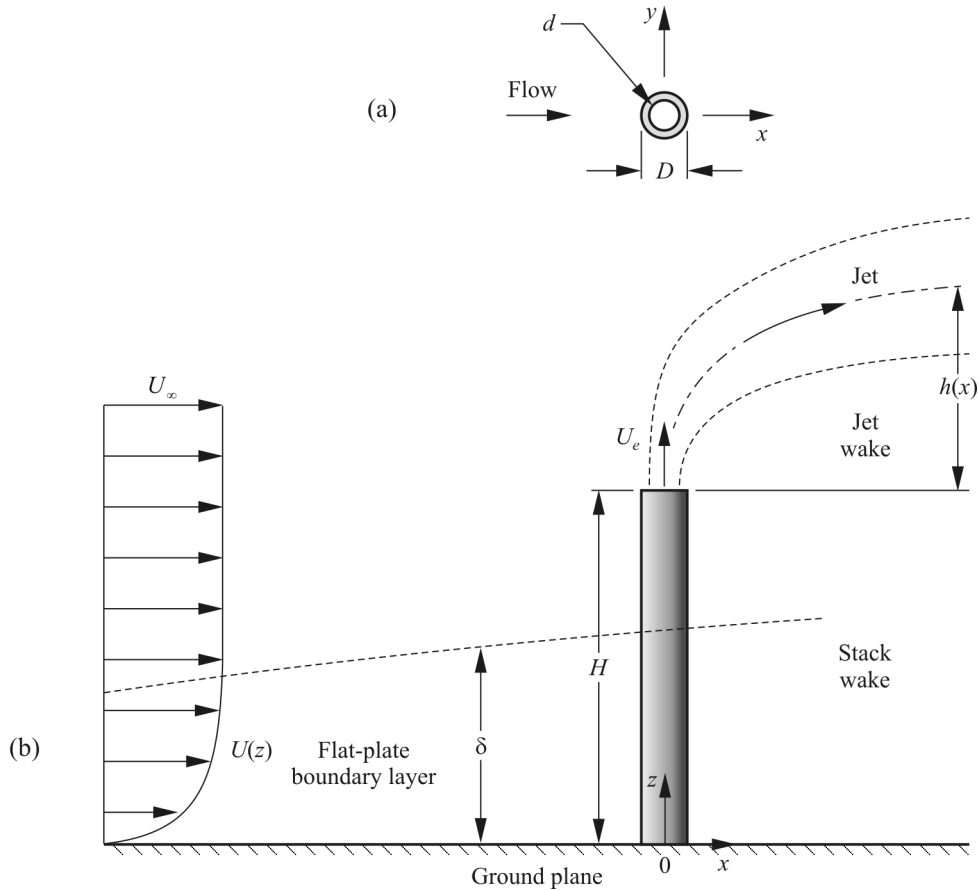
Figure 1. Stack of uniform circular cross-section (of diameter, D, and height, H) mounted normal to a ground plane and partially immersed in a turbulent flat-plate boundary layer (of thickness, δ, and freestream velocity, U_∞): (a) top view; (b) side view.

wash" velocity field is found between the base vortex structures closer to the ground plane [1, 11]. A localized region of low mean streamwise velocity and high turbulence intensity is found behind the cylinder, centred between the four main streamwise vortex structures [1].

The presence of a jet issuing from a cylindrical stack (Figure 1) makes the wake of the stack more complex compared with the finite cylinder. For a non-buoyant jet, the extent of this complexity depends primarily on the jet-to-cross-flow velocity ratio, R (= U_e/U_∞, where U_e is the average jet exit velocity and U_∞ is the freestream velocity outside the boundary layer on the ground plane).

The local flow field of the stack is characterized by the complex interactions between the jet and stack wake regions, shear produced by the upward momentum of the jet, and downwash flow [2, 3, 4, 5, 6, 7, 8]. Studies of the flow topology in the vertical plane along the stack wake centreline (the x-z plane, Figure 1b) have been used to classify the stack and jet wake flow patterns into a number of flow regimes based on the approximate value of R [5, 6, 8]. Studies of a high-aspect-ratio stack (AR = 25) [5, 6], for example, have identified four flow regimes: (i) downwash flow ($R < 0.95$), (ii) cross-wind-dominated flow ($0.95 < R <$

1.4), (iii) transitional flow (1.4 < R < 2.4), and (iv) jet-dominated flow (R > 2.4). A similar study of the local flow field of a small-aspect-ratio stack (AR = 8.3) [8] identified three zones within the jet: zone 1, immediately above the stack exit, where the jet dominates the flow; zone 2, where the jet begins to bend and the jet flow and cross-flow have the same velocity; and zone 3, further downstream, where the cross-flow dominates the flow. Depending on the value of R and the corresponding flow regime, one or more of these zones may be absent.

In a more recent study of a small-aspect-ratio stack (AR = 9) partially immersed in a flat-plate turbulent boundary layer [2], wake velocity measurements were made in cross-stream (y-z) planes for jet-to-cross-flow velocity ratios ranging from R = 0 to 3. The near-field behaviour of the stack was broadly classified into three flow regimes; adopting the terminology used by [5, 6], these flow regimes were classified as the downwash (R < 0.7), cross-wind-dominated ($0.7 \leq R$ < 1.5), and jet-dominated ($R \geq 1.5$) flow regimes. Each flow regime had a distinct structure to the mean velocity field, turbulence intensity field, and Reynolds stresses [2].

The influence of the jet-to-cross-flow velocity ratio, R, on the streamwise vortex structures has not been extensively investigated. These structures are known to have an important role in the problem of stack downwash [7], which occurs at low jet-to-cross-flow velocity ratios. In the present study, the behaviour of the streamwise vortex structures in the near-field of a small-aspect-ratio (AR = 9) stack is investigated for a range of jet-to-cross-flow velocity ratios.

2. Experimental Approach

The experimental set-up was similar to that adopted by [2]. The experiments were conducted in a low-speed, closed-return wind tunnel with a test section of 0.91 m (height) × 1.13 m (width) × 1.96 m (length). The longitudinal freestream turbulence intensity was less than 0.6% and the velocity non-uniformity outside the test section wall boundary layers was less than 0.5%.

The test section floor was fitted with a ground plane. A rough strip located about 200 mm from leading edge of the ground plane was used to produce a turbulent flat-plate boundary layer on the ground plane at the location of the stack.

2.1. EXPERIMENTAL APPARATUS

A cylindrical stack of H = 171.5 mm, D = 19.1 mm, d/D = 0.67 (where d is the internal diameter, see Figure 1), and AR = 9, was used in the present study. The experiments were conducted at a freestream velocity of U_∞ = 20 m/s, giving a Reynolds number, based on the stack external diameter, of Re_D = 2.3×10^4. The solid blockage ratio was 0.3% and no wall interference corrections were made.

The stack was located 700 mm downstream of the rough strip on the ground plane. At the location of the stack, the boundary layer thickness was $\delta = 83$ mm, the boundary layer shape factor was 1.3, and the Reynolds number based on momentum thickness, θ, was $Re_\theta = 0.86 \times 10^4$. This boundary layer provided a thickness-to-height ratio of $\delta/H \approx 0.5$ at the location of the stack.

A pair of screens was installed at the stack supply inlet to ensure the flow exiting the stack was turbulent. The mean axial velocity profiles at the stack jet exit were similar to the typical velocity profile for a turbulent pipe flow. The exhaust velocity of the non-buoyant stack jet was varied with two MKS 1559A-200L mass flow controllers arranged in parallel. The jet-to-cross-flow velocity ratio was varied from $R = 0$ (no jet exiting the stack) to $R = 3$, corresponding to momentum flux ratios of $R_m = 0$ to 9. The jet Reynolds number for the minimum exit velocity, when $R = 0.5$, was $Re_d = 7.6 \times 10^3$ (based on the internal diameter of the stack, d, and the average jet exit velocity, U_e). The jet Reynolds number for the maximum exit velocity, when $R = 3$, was $Re_d = 4.7 \times 10^4$.

2.2. MEASUREMENT INSTRUMENTATION

The wind tunnel data were acquired with a personal computer, a National Instruments PCI-6031E 16-bit data acquisition board, and LabVIEW software. The freestream conditions were obtained with a Pitot-static probe (United Sensor, 3.2-mm diameter), Datametrics Barocell absolute and differential pressure transducers, and an Analog Devices AD590 integrated circuit temperature transducer.

Wake measurements were made with a seven-hole pressure probe (3.45-mm diameter, 30° cone angle). The seven pressures were measured with a Scanivalve ZOC-17 pressure scanner. The probe was calibrated in situ using an automated variable-angle calibrator, with a calibration grid spacing of 8.1° over a flow angle range of ± 72.9°. A direct-interpolation calibration data-reduction method was used [10]. The measurement uncertainty was estimated to be less than 3° for the flow angle and less than 5% for the velocity magnitude.

The seven-hole probe was mounted in a three-axis, computer-controlled traversing system. For each value R, the time-averaged wake velocity field (u, v, w components) in the cross-stream (y-z) plane was measured over a 5-mm uniform grid at streamwise locations from $x/D = 6$ to 10 downstream of the stack. From each velocity field, the time-averaged streamwise vorticity field, $\omega_x(y, z)$, was determined. In addition, the wake velocity field was measured in a vertical (x-z) plane parallel to the test-section centreline (at $y/D = 0$).

3. Results and Discussion

Results are presented for three values of the jet-to-cross-flow velocity ratio, R, each value representing one of the three flow regimes identified by [2]: $R = 0.5$
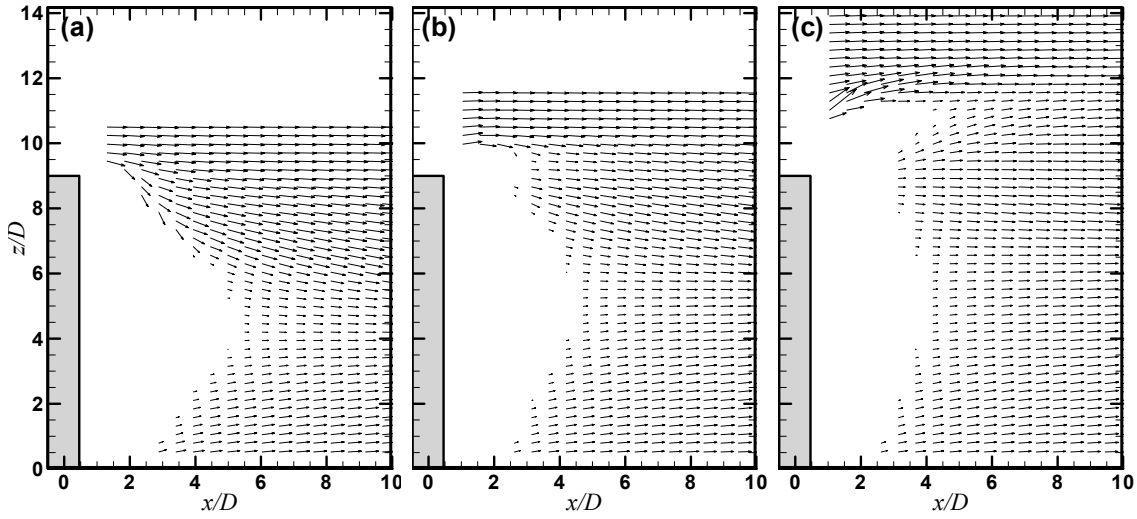
Figure 2. The time-averaged velocity vector field along the wake centreline (*y/D* = 0) for the (a) downwash flow regime, *R* = 0.5; (b) cross-wind-dominated flow regime, *R* = 1; and (c) jet-dominated flow regime, *R* = 2.5.

(downwash flow regime), *R* = 1 (cross-wind-dominated flow regime) and *R* = 2.5 (jet-dominated flow regime). Similar to the definition of [4], the stack wake is defined as the region below the free end, where $0 < z/H \leq 1$ $(0 < z/D \leq 9)$, and the jet wake is defined as the region above the free end, where $z/H > 1$ $(z/D > 9)$.

3.1. TIME-AVERAGED VELOCITY FIELDS ON THE WAKE CENTRELINE

Time-averaged velocity vector fields in the vertical (*x-z*) plane along the wake centreline (at *y/D* = 0) are shown in Figure 2 for three values of *R*. In each case, immediately behind the stack is a region of highly angled or recirculating flow, indicated by an absence of velocity vectors. The absence of vectors in this region indicates that the local flow angle exceeded the angular range of the seven-hole probe, which was estimated at $\pm 70°$ [10, 11]. For each value of *R*, the streamwise extent of this recirculation region varies along the stack height.

For *R* = 0.5 (Figure 2a), which represents the downwash flow regime, the downwash flow (downward-directed velocity) is observed within the stack wake close to the stack's free end. This downwash flow persists in the streamwise direction and descends from the free end towards the mid-height of the stack. An upwash flow (upward-directed velocity) is observed near the base of the stack and within the flat-plate boundary layer on the ground plane. These downwash and upwash flows are similar to the case of the finite circular cylinder [11, 12], which corresponds to the case of *R* = 0. However, with the presence of the weak jet flow exiting the stack at *R* = 0.5, the strength of the downwash flow, and the streamwise and vertical extents of the upwash flow, are reduced compared to the finite circular cylinder. In addition, the maximum streamwise extent of the recir-

culation region is smaller, while closer to the stack free end the length of the re-circulation region is greater, compared to finite-cylinder ($R = 0$) case.

For $R = 1$ (Figure 2b), which corresponds to the cross-wind-dominated flow regime, the downwash flow is absent in the near-wake region of the stack. Compared to $R = 0.5$ (Figure 2a), the streamwise extent of the upwash flow is reduced but it now extends to a greater vertical distance above the ground plane. In addition, for $R = 1$ (Figure 2b), the maximum streamwise extent of the recirculation region within the stack wake is smaller, but a more sizeable recirculation region is now found in the vicinity of the stack free end. This is caused by the stronger jet flow, which now behaves more like a bluff body. Another recirculation region is also observed above the free end of the stack and within the jet wake. This region may contain the vortex formed within the jet wake as observed by [5] for $0.95 < R < 2.4$, which is due to the presence of the jet flow.

For $R = 2.5$ (Figure 2c), which corresponds to the jet-dominated flow regime, the stronger momentum of the jet flow allows it to penetrate the cross-flow, as shown by the upward-directed velocity vectors above the free end of the stack. With the increased jet rise, the size of the recirculation region within the jet wake is now larger compared to the cross-wind-dominated flow regime at $R = 1$ (Figure 2b). A strong recirculation region within the jet wake was also observed by [8]. There is also a corresponding reduction in the size of the recirculation region within the stack wake, and the streamwise extent of this region becomes more uniform along the stack height.

3.2. TIME-AVERAGED CROSS-STREAM VELOCITY FIELDS

Time-averaged cross-stream velocity vector fields (v, w velocity components measured in the y-z plane) at $x/D = 6$ are presented in Figure 3 for the same three values of R as in Figure 2. For the downwash flow regime (Figure 3a, $R = 0.5$) and the cross-wind-dominated flow regime (Figure 3b, $R = 1$), the vector fields show two pairs of counter-rotating velocity fields within the stack wake, one closer to the free end and the other closer to the ground plane. For the jet-dominated flow regime (Figure 3c, $R = 2.5$), an additional pair is observed in the jet wake region. For all of the three flow regimes, the upwash flow is observed within the flat-plate boundary layer on the ground plane near the stack base. The strength of this upwash flow is strongest within the boundary layer and reduces towards the mid-height of the stack.

For $R = 0.5$ (Figure 3a), there is a presence of strong a downwash flow within the stack wake and below the stack free end, which is the main characteristic of the downwash flow regime. The strength of the downwash flow reduces along the height of the stack when moving away from the free end and towards the base, similar to the case of the finite circular cylinder [11].

For $R = 1$ (Figure 3b), representing the cross-wind-dominated flow regime, the downwash velocity field is located further away from the ground plane and
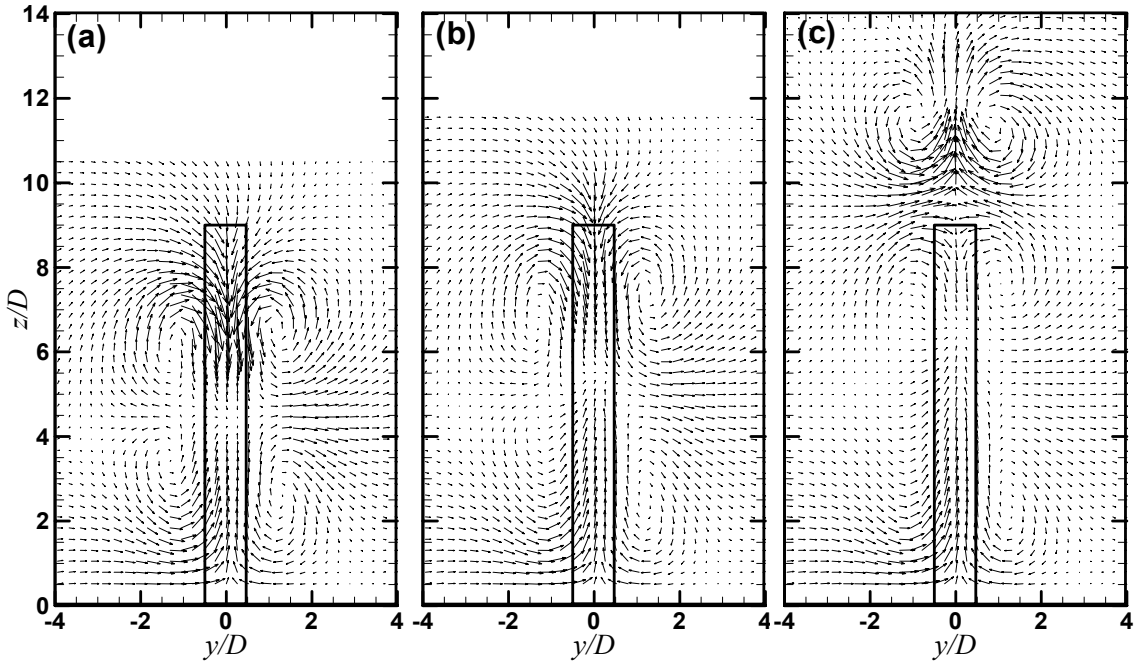
Figure 3. The time-averaged velocity vector field downstream of the stack at $x/D = 6$ for the (a) downwash flow regime, $R = 0.5$; (b) cross-wind-dominated flow regime, $R = 1$; and (c) jet-dominated flow regime, $R = 2.5$.

closer to the stack's free end. The downwash for $R = 1$ is weaker than for $R = 0.5$ (Figure 3a). In addition, for the same streamwise position, the upper pair of two the counter-rotating velocity fields now occurs closer to the free end of the stack.

For $R = 2.5$ (Figure 3c), a second and much stronger upwash flow occurs above the free end of the stack within the jet wake region. This upwash extends more than 4 stack diameters above the free end, and is associated with the third pair of the counter-rotating velocity fields. These features characterize the jet-dominated flow regime and result from the stronger jet flow exiting the stack.

3.3. TIME-AVERAGED STREAMWISE VORTICITY FIELDS

The time-averaged streamwise vorticity ($\omega_x^* = \omega_x D/U_\infty$, where ω_x is the streamwise vorticity component) fields in the *y-z* plane at $x/D = 6$ are shown in Figure 4 for the same three values of R as in Figures 2 and 3. For each of the three flow regimes, the streamwise vorticity field shows two counter-rotating vortex pairs within the stack wake: one pair near the stack free end, referred to as the "tip vortex pair", and another of opposite sense of rotation closer to the base of the stack, referred to as the "base vortex pair." These two pairs of vortex structures were evident in the mean cross-stream velocity vector fields, shown in Figure 3, and are also observed in the wake of a finite circular cylinder [11, 12]. The tip vortex structures are stronger than the base vortex structures, consistent with [11, 12].
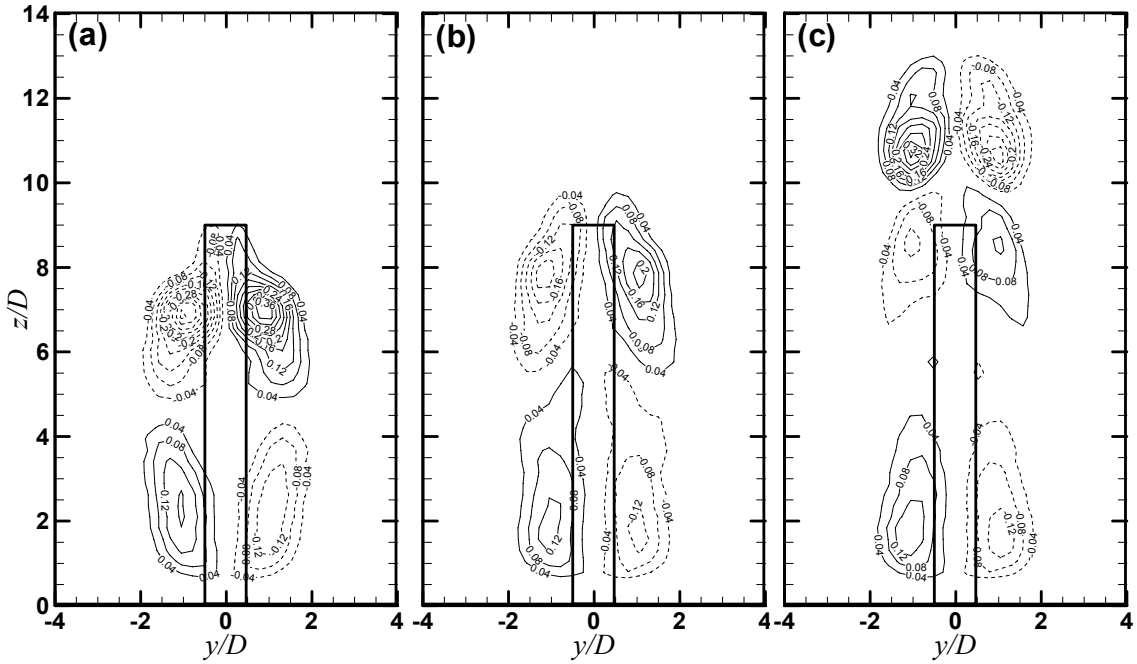
Figure 4. The time-averaged streamwise vorticity field downstream of the stack at $x/D = 6$ for the (a) downwash flow regime, $R = 0.5$; (b) cross-wind-dominated flow regime, $R = 1$; and (c) jet-dominated flow regime, $R = 2.5$. Iso-vorticity contour lines of $\omega_x{}^*$. Solid lines represent positive (CCW) vorticity; dashed contour lines represent negative (CW) vorticity; minimum vorticity contour of $\omega_x{}^* = \pm\, 0.04$; contour increment of $\Delta\omega_x{}^* = 0.04$.

In the downwash flow regime (Figure 4a, $R = 0.5$), the tip vortex pair at $x/D = 6$ is located below the free end, similar to the finite cylinder [11, 12]. In the cross-wind-dominated flow regime (Figure 4b, $R = 1$), the tip vortex pair now extends above the free end. In addition, the base vortex structures are stretched upward along the sides of the stack towards the mid-height position.

In the jet-dominated flow regime (Figure 4c, $R = 2.5$), the tip vortex pair has weakened considerably compared to the downwash and cross-wind-dominated flow regimes (Figures 4a and 4b, respectively). In addition to the two pairs of streamwise vortex structures found within the stack wake region, a third counter-rotating vortex pair is now found in the jet wake region. Evidence of this vortex pair was seen in the velocity vector field (Figure 3c). This third vortex pair, referred to as the "jet-wake vortex pair", is located above the free end of the stack and is similar to the kidney-type vortex pair observed for a bent jet in cross-flow. The sense of rotation of the jet-wake vortex pair is the same as the base vortex pair but opposite to the tip vortex pair. The jet-wake vortex structures are associated with the jet rise and the strong upwash velocity field above the free end of the stack (Figure 3c), and are stronger than the tip vortex structures.

The streamwise development of the vortex structures in the jet-dominated flow regime is presented in Figure 5, for $x/D = 6$ to 10. The size and strength of the tip and jet-wake vortex pairs decrease with increasing distance from the stack. The behaviour of the weaker base vortex pair with x/D is more irregular.
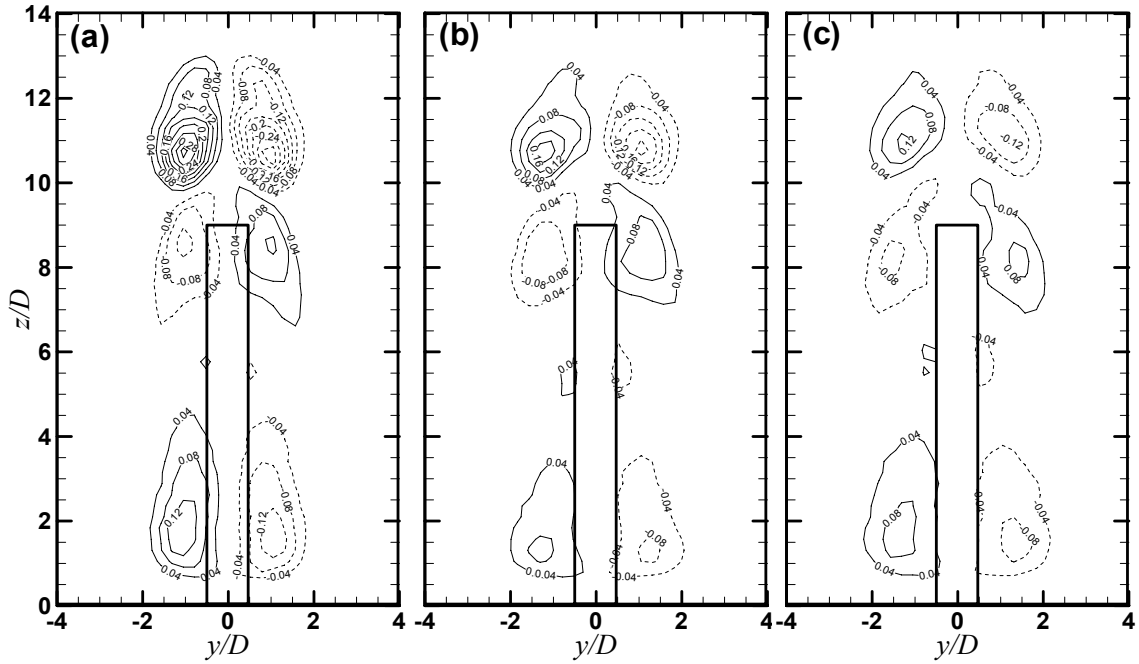
Figure 5. Streamwise development of the time-averaged streamwise vorticity field behind the stack for $R = 2.5$: (a) $x/D = 6$; (b) $x/D = 8$; and (c) $x/D = 10$. Contour lines as in Figure 4.

4.   Conclusions

In the present study, a seven-hole pressure probe was used to measure the time-averaged velocity and streamwise vorticity fields in the wake of a stack operating at jet-to-cross-flow velocity ratios from $R = 0$ to 3. This range of velocity ratio covered the three main flow regimes describing the fluid behaviour close to the stack, namely the downwash, cross-wind-dominated, and jet-dominated flow regimes. As R is varied, marked changes occur in the downwash and upwash velocity fields, the location, strength, and number of streamwise vortex structures, and the size and shape of the recirculation zone in the near wake of the stack.

In the downwash flow regime, the flow is similar to that of a finite circular cylinder, with two pairs of counter-rotating streamwise vortex structures, each of opposite sign, in the stack wake. The tip vortex pair is found closer to the free end of the stack and is associated with a strong downwash velocity field immediately behind the stack. The weaker base vortex pair is found within the flat-plate boundary layer on the ground plane and is associated with an upwash velocity field directed away from the ground plane.

In the cross-wind-dominated flow regime, the tip vortex pair extends just above the free end of the stack and base vortex pair is stretched vertically towards the mid-height of the stack. The downwash and upwash velocity fields, and the vortex pairs, are weakened compared to the downwash flow regime.

For the jet-dominated flow regime, three pairs of counter-rotating streamwise vortex structures are observed. In addition to the tip vortex and base vortex pairs found at lower velocity ratios, the jet-wake vortex pair appears in the jet wake

region above the free end of the stack. The jet-wake vortex pair is associated with the jet rise and a strong upwash velocity on the jet wake centreline.

Acknowledgments

References

1. Adaramola, M.S., Akinlade, O.G., Sumner, D., Bergstrom, D.J., and Schenstead, A.J., Turbulent wake of a finite circular cylinder of small aspect ratio. *J. Fluid Struct.* **22** (2006) 919-928.
2. Adaramola, M.S., Sumner, D., and Bergstrom, D.J., Turbulent wake of a stack and the influence of velocity ratio. Proceedings of the 6th International Symposium on Fluid-Structure Interactions, Aeroelasticity, Flow-Induced Vibration & Noise, Vancouver, Canada, ASME PVP Division, July 23-27, 2006, Paper No. PVP2006-ICPVT11-93629 (2006) 1-9.
3. Eiff, O.S., Kawall, J.G., and Keffer, J.F., Lock-in of vortices in the wake of an elevated round turbulent jet in a crossflow. *Exp. Fluids* **19** (1995) 203-213.
4. Eiff, O.S. and Keffer, J.F., Parametric investigation of the wake-vortex lock-in for the turbulent jet discharging from a stack. *Exp. Therm. Fluid Sci.* **19** (1999) 57-66.
5. Huang, R.F. and Hsieh, R.H., An experimental study of elevated round jets deflected in a crossflow. *Exp. Therm. Fluid Sci.* **27** (2002) 77-86.
6. Huang, R.F. and Hsieh, R.H., Sectional flow structures in near wake of elevated jet in a crossflow. *AIAA J.* **41** (2003) 1490-1499.
7. Johnston, C.R. and Wilson, D.J., A vortex pair model for plume downwash into stack wakes. *Atmos. Environ.* **31** (1997) 13-20.
8. Mahjoub Saïd, N., Mhiri, H., Le Palec, G., and Bournot, P., Experimental and numerical analysis of pollutant dispersion from a chimney. *Atmos. Environ.* **39** (2005) 1727-1738.
9. Okamoto, S., Flow past circular cylinder of finite length placed on ground plane. *Trans. Jpn. Soc. Aeronaut. Space Sc.* **3**3 (1991) 234-246.
10. Sumner, D., A comparison of data-reduction methods for a seven-hole probe. *J. Fluid Eng.-T. ASME* **124** (2002) 523-527.
11. Sumner, D., Heseltine, J.L., and Dansereau, O.J.P., Wake structure of a finite circular cylinder of small aspect ratio. *Exp. Fluids* **37** (2004) 720-730.
12. Tanaka, S. and Murata, S., An investigation of the wake structure and aerodynamic characteristics of a finite circular cylinder. *JSME Int. J. B-Fluid T.* **42** (1999) 178-187.